Structural Properties of Self-Organized Organo-Silicon Macromolecular Films Investigated by Scanning Tunneling Microscopy and X-ray Diffraction

P. Miao, A. W. Robinson, and R. E. Palmer*

Nanoscale Physics Research Laboratory, School of Physics and Astronomy, University of Birmingham, Birmingham B15 2TT, U.K.

B. M. Kariuki and K. D. M. Harris*,†

School of Chemistry, University of Birmingham, Birmingham B15 2TT, U.K.

Received: September 8, 1999; In Final Form: November 30, 1999

Scanning tunneling microscopy (STM) and scanning tunneling spectroscopy (STS) have been applied to investigate thin films of a model silicon-containing macromolecule, silicon phthalocyanine dichloride ($SiPcCl_2$), deposited from solution on to the H-passivated Si(111) surface. In a high coverage film, clusters of about 5.5 nm × 4.5 nm in size are observed. These clusters are believed to partially stack on each other, suggesting a tilted growth mechanism of the layers on the surface. In a low coverage film, well-ordered monolayers are found, with a close structural similarity to the bulk crystal structure of $SiPcCl_2$. In this work, the bulk crystal structure of $SiPcCl_2$ was determined directly from powder X-ray diffraction data using the Monte Carlo method. The results of STM manipulation and the observation of well-ordered $SiPcCl_2$ layers on the Si(111) surface indicate a weaker interaction between the $SiPcCl_2$ molecules and the substrate than between the $SiPcCl_2$ molecules. STS measurements show rectifying behavior which is attributed to the H-passivated silicon surface.

1. Introduction

The structural properties of macromolecular films composed of phthalocyanine (abbreviated Pc) molecules[1,2] and the structures of the bulk crystals[3−5] have attracted considerable interest. Underlying this interest is the fact that thin films of phthalocyanines have shown considerable promise in a number of areas of application, such as solar cells,[6] transistors,[7] and light emitting devices.[8] The performance of these devices has been found to vary considerably, depending on the structure of the films deposited on surfaces. For example, nonlinear optical properties depend both on the quality of the structure and the molecular alignment within the structure.[9] The electrical properties, such as extrinsic conductivity, of thin films can be improved by morphological changes from granular discontinuous films to uniform continuous films.[10] Studies of the structural properties and manipulation of these molecules deposited as thin films on surfaces are clearly prerequisites for understanding the fundamental physical and electronic properties of the devices. The uses of phthalocyanines extend beyond such devices, and several applications based on their optical properties and thermal stability have been developed.[11,12] Thus, phthalocyanines are used as dyes[13] and as potential photosensitizers in photodynamic therapy of cancer.[14−16] Phthalocyanines can also be used as precursors to prepare high quality oxide thin films which cannot be obtained easily using conventional metal−organic compounds in metal−organic chemical vapor deposition (MO-CVD), MO molecular beam epitaxy (MO-MBE), and chemical beam epitaxy (CBE).[17]

Scanning tunneling microscopy (STM) has been used widely to study phthalocyanine derivatives on several different surfaces, as it can provide a direct view of the molecular structure and adsorption geometry. Metal phthalocyanines such as copper (CuPc),[18−23] lead (PbPc),[24] cobalt (CoPc), iron (FePc), and nickel (NiPc)[25] phthalocyanines have been widely studied in this regard. Tanaka and co-workers[21] observed that planar CuPc molecules are bonded in a stable manner on the $SrTiO_3$ surface in ultrahigh vacuum (UHV), whereas CuPc can diffuse on the much less chemically active Cu(111) surface to create low-dimensional structures. Maeda et al.[19] and Kanai et al.[23] obtained similar results in UHV, showing that CuPc molecules have three adsorption configurations on the dimer row of Si(100) with the molecular plane parallel to the surface, dominated by the interaction between the aromatic rings of CuPc molecules and Si dangling bonds. Kanai et al.[23] also observed a distinctive bias-voltage dependence of the STM images of CuPc molecules on Si(111) in UHV, suggesting that there is a strong interaction between the molecule and the surface. On the H-passivated Si(111) surface, the stacking and orientation of CuPc in UHV was found to be affected by the surface roughness.[18] On a rough surface, the CuPc molecules are stacked with the molecular columns parallel to the surface, whereas on an atomically flat surface, the CuPc molecules are stacked in columns perpendicular to the surface. Nonplanar PbPc molecules were found[24] to have three adsorption phases on MoS_2 in UHV, instead of the two phases observed for CuPc on the same surface. For CuPc, a close-packed phase with a square unit cell and a row-like phase were observed. For PbPc, the additional adsorption phase comprised three adjacent close-packed rows separated by one or two isolated single rows. Molecularly resolved images of PbPc on MoS_2 show two different adsorption geometries, with the Pb atom above or below the Pc plane (the molecule is nonplanar). Interestingly, CuPc was also found[2] to induce faceting of misoriented Ag(110).

* Authors to whom correspondence should be addressed.
† E-mail: K.D.M.Harris@bham.ac.uk.

10.1021/jp993167r CCC: $19.00
Published on Web 01/25/2000

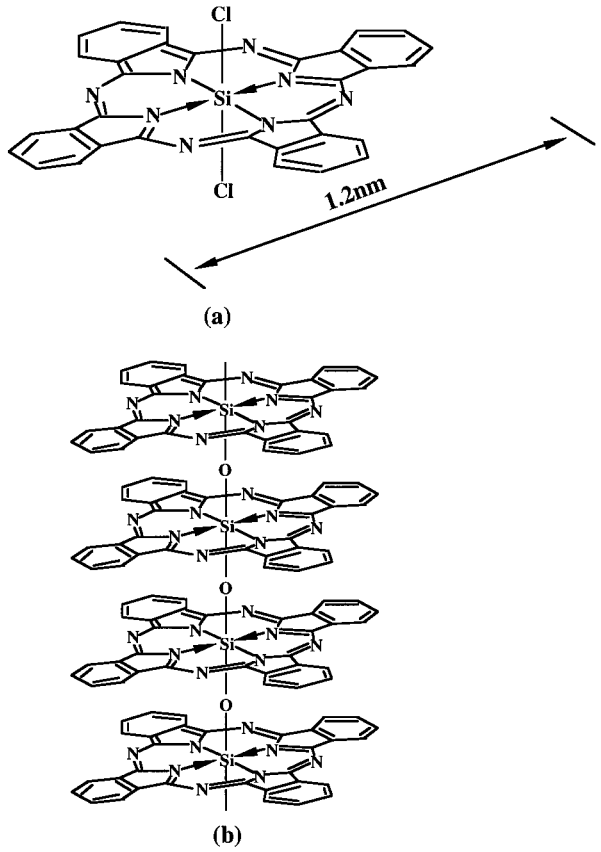

Figure 1. (a) Molecular structure of silicon phthalocyanine dichloride ($SiPcCl_2$). The lateral dimension in the plane of the phthalocyanine molecule is about 1.2 nm. (b) The $(SiPcO)_n$ chain after polymerization of $SiPc(OH)_2$.

In addition to STM studies, X-ray diffraction methods have also been used to determine the structures of phthalocyanines deposited on surfaces or in the bulk.[26,3−5] These reports demonstrate that the thin films of phthalocyanine molecules may take up a variety of stacking arrangements on the surface, which depend not only on the morphology of the surface but also on the structure of the molecule and its preferred modes of stacking (as evidenced from the crystal structure).

In the context of nanoscale science and technology, we are interested in silicon phthalocyanine dichloride [$Si(C_{32}H_{16}N_8)Cl_2$; abbreviated $SiPcCl_2$] as the precursor of a conducting polymer which has applications as an electronic or photoelectronic material; strands of this polymer could be used to create nanoscale electrical connections and other functional nanostructures for electronic devices. In the molecular structure of $SiPcCl_2$ (Figure 1a), a Si atom is located at the center of the planar phthalocyanine (Pc) ring, with two Cl atoms attached to the Si atom above and below the SiPc plane. The polymerization procedure is briefly summarized as follows.[27] In the first step, the chlorine atoms above and below the SiPc plane are replaced by hydroxyl (OH) groups. In the second step, a water molecule is eliminated between hydroxyl groups of adjacent $SiPc(OH)_2$ molecules, leading to the formation of a Si−O−Si linkage. As there are two OH groups per $SiPc(OH)_2$ molecule, this dehydration reaction leads to polymer formation, as shown in Figure 1b.

From the viewpoint of fabrication of single conducting polymer strands, a particularly attractive route would be to position the precursor $SiPcCl_2$ molecules on a surface and then to carry out in situ hydrolysis and polymerization to form the conducting polymer. Thus, it is important to understand (1) how the $SiPcCl_2$ molecule interacts with the surface, (2) the types of structures that form naturally when $SiPcCl_2$ is deposited from solution, and (3) whether thin films of $SiPcCl_2$ suitable for fabricating electrical connecting strands may be manipulated using the STM tip (in order to position molecules prior to polymerization). We have already reported manipulation of thick films of $SiPcCl_2$ using STM.[28] In this paper, we explore the behavior of $SiPcCl_2$ on the H-passivated Si(111) surface using STM and scanning tunneling spectroscopy (STS) operated in air. The interaction between the molecules and the surface, the surface morphology, and the behavior of the I−V curve are discussed. In studies of adsorbates on surfaces, it is important to compare the surface structure with the structure of the bulk material, and the crystal structure of $SiPcCl_2$ has been determined in this work. Single crystals of $SiPcCl_2$ of appropriate size and quality for conventional single crystal X-ray diffraction studies were not available, and structure determination was carried out by taking advantage of recent developments in the methodology for solving crystal structures directly from powder diffraction data.

Structure solution from powder diffraction data[29] is associated with intrinsic difficulties originating from the fact that, in a powder diffraction pattern, three-dimensional diffraction data (as for a single crystal) are compressed into one dimension. As a consequence, the peaks in a powder diffraction pattern usually overlap considerably, which can lead to difficulties in extracting reliable values for the intensities $I(hkl)$ of individual diffraction maxima directly from the experimental data. Nevertheless, the traditional approach for solving crystal structures from powder diffraction data has been to attempt to extract such integrated intensities from the experimental data, and then to use these integrated intensities in the types of structure solution calculations that are used routinely for single-crystal diffraction data (e.g., direct methods or the Patterson method[29]). An alternative strategy (the "direct-space" approach) for solving structures from powder diffraction data involves the generation of trial structures in direct space, with the quality of each trial structure assessed by directly comparing the powder diffraction pattern calculated for the trial structure and the experimental powder diffraction pattern. Most direct-space approaches, including the method described in this paper, have used the weighted profile R-factor[29] R_{wp} (the R-factor normally used in Rietveld refinement) to assess the agreement between calculated and experimental powder diffraction patterns. R_{wp} considers the whole digitized intensity profile directly "as measured", rather than the integrated intensities $I(hkl)$ of individual diffraction maxima, and thus takes implicit consideration of peak overlap. Within direct-space strategies, a number of different methods have been used to generate trial crystal structures, including Monte Carlo sampling,[30−32] simulated annealing[33−35] and genetic algorithms.[36−39] In the present work, the Monte Carlo technique[30] with Metropolis importance sampling applied on the basis of R_{wp} has been used to solve the crystal structure of $SiPcCl_2$.

2. Experimental Section

Hydrogen-passivated Si(111) surfaces were prepared from commercial p-type Si(111) wafers (boron-doped, 1−2 ohm.cm, from Virginia Semiconductor, Inc.). These were first cut into 10 mm × 10 mm squares, and then passivated with hydrogen using the procedure reported previously.[40] The preparation of the H-passivated Si(111) surface is now summarized briefly. First, the samples were degreased successively in trichloroethylene at 80 °C for 10 min, in acetone at room temperature for

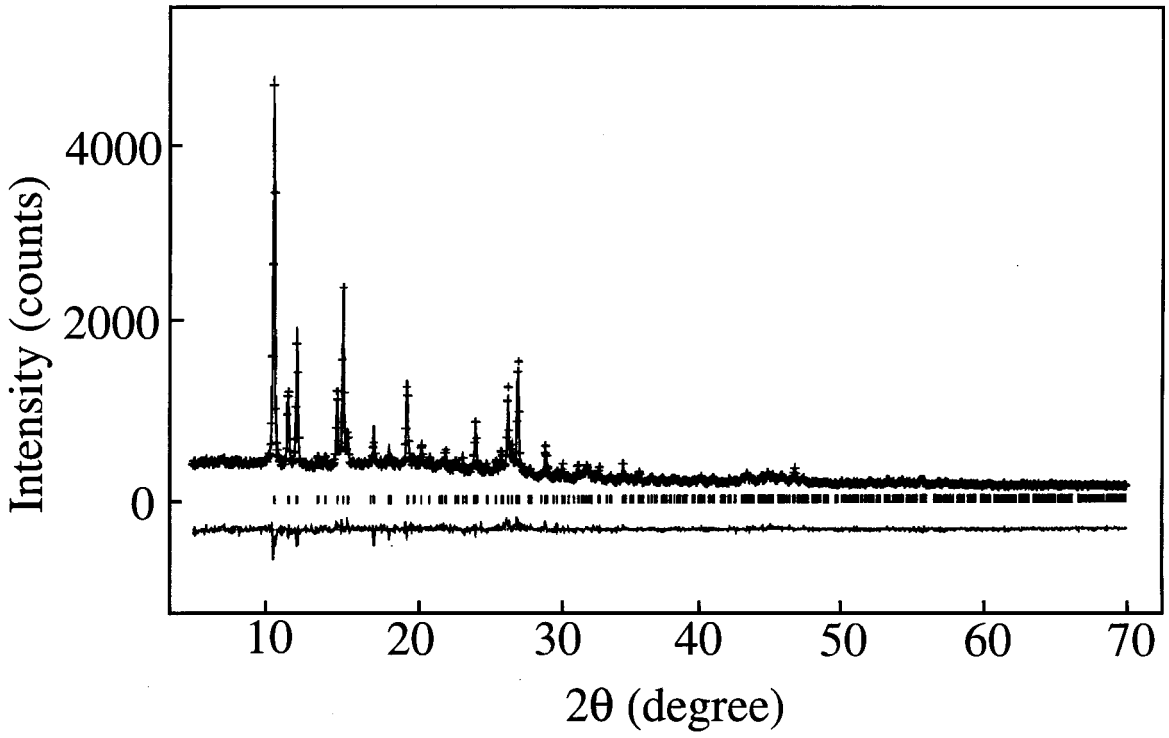

Figure 2. Experimental (+ marks), calculated (solid line), and difference (lower line) power X-ray diffraction profiles for the Rietveld refinement of $SiPcCl_2$. Reflection positions are marked. The calculated powder diffraction profile is for the final refined crystal structure, details of which are given in Table 1.

10 min, and in methanol at room temperature for 10 min, followed by a thorough spray-rinse with ultrapure deionized water ($\rho > 18$ MΩ) for 1 min. Then, the samples were oxidized in a mixed solution (1:1 ratio) of 98% H_2SO_4 and 30% H_2O_2 at 80 °C for 10 min. After this oxidation step, the samples were thoroughly spray-rinsed again with deionized water for 1 min, and then immediately etched in 40% NH_4F solution for 20 min at room temperature. Finally, these samples were quickly spray-rinsed with deionized water for 15 s and dried in air. $SiPcCl_2$ powder (Aldrich) was first dissolved in trichloroethylene (99+ %; Aldrich) to make a saturated solution, which was then further diluted with trichloroethylene (1:3 ratio of saturated solution to solvent). The $SiPcCl_2$ deposited samples were prepared by spreading a droplet of this solution on the freshly H-passivated Si(111) substrates, then covering with a glass beaker (which slows down the evaporation of trichloroethylene in air) and leaving to dry for 1 h.

The benchtop STM employed was a Rasterscope 4000 (Danish Micro Engineering) with Pt−Ir tips. The STM was operated in a constant current mode in air. All images were taken after the samples had been allowed to dry in air for 1 h. Scanning tunneling spectroscopy (STS) I−V curves were measured at various points via a single point spectroscopic measurement at a constant height.

The powder X-ray diffraction pattern of $SiPcCl_2$ was recorded at 295 K on a Siemens D5000 diffractometer, using Ge-monochromated $CuK_{\alpha 1}$ radiation and a linear position-sensitive detector covering 8° in 2θ. The total 2θ range was 5° to 70°. The powder diffraction pattern was indexed using the program ITO,[41] giving the monoclinic unit cell: $a = 1.03$ nm, $b = 1.46$ nm, $c = 0.90$ nm, $\beta = 98.3°$. Systematic absences were consistent with space group $P2_1/n$, and density considerations indicated that there are two molecules in the unit cell (i.e., the asymmetric unit comprises half of the $SiPcCl_2$ molecule). Structure solution by the Monte Carlo method was carried out using the program OCTOPUS,[42] and structure refinement by the Rietveld method was carried out using the GSAS program package.[43]

3. Results

3.1. Structure Determination of Bulk $SiPcCl_2$. In the Monte Carlo structure solution calculation, the structural fragment comprised half of the centrosymmetric $SiPcCl_2$ molecule (with hydrogen atoms omitted) and was constructed using bond distance and bond angle information from the known structures of other phthalocyanine derivatives in the Cambridge Structural Database.[44] In the structure solution calculation, the silicon atom was placed on the center of inversion, and the structural fragment was subjected to rotation about this point under the control of the Monte Carlo algorithm. Each move involved rotation of the fragment about three mutually perpendicular axes in orthogonal space. The maximum displacement about each axis was 180° and the value of the scaling parameter S[29,30] was 3. In total, 2000 Monte Carlo moves were considered. The average value of R_{wp} for trial structures was 37.2% and the maximum value of R_{wp} was 41.9%. The value of R_{wp} for the best structure solution (lowest R_{wp}) was 23.6%.

Structure refinement was carried out using the Rietveld profile refinement method, taking the best structure solution from the Monte Carlo calculation as the initial structural model. Throughout the refinement, bond distances were restrained to standard values[45] and all isotropic displacement parameters were fixed at 0.025 Å^2. Hydrogen atoms were not included in the refinement. The agreement factors for the final refined structure were $R_{wp} = 9.2\%$ and $R_p = 7.4\%$. The experimental and calculated powder X-ray diffraction patterns are compared in Figure 2. Atomic coordinates for the final refined structure are given in Table 1. In the final refined crystal structure (Figure 3), the planes of the $SiPcCl_2$ molecules lie close to the *bc* plane, with each molecule tilted away from this plane by approximately 20°. The Si−Cl bonds are directed roughly parallel to the *a*

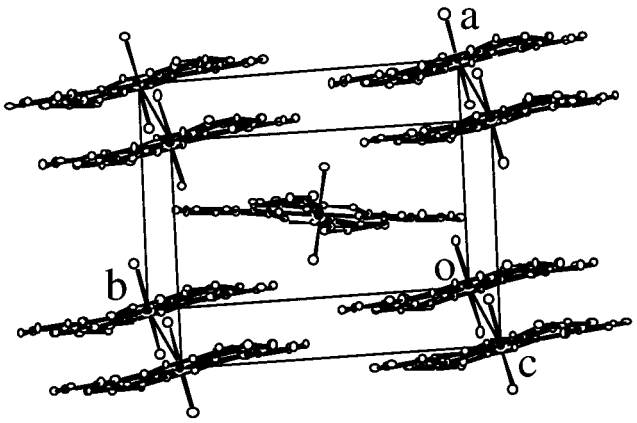

Figure 3. Final refined crystal structure of $SiPcCl_2$ (hydrogen atoms not shown). The unit cell dimensions are $a = 1.03$ nm, $b = 1.46$ nm, $c = 0.90$ nm, $\beta = 98.4°$.

TABLE 1: Fractional Atomic Coordinates for the Crystal Structure of $SiPcCl_2$ at 295 K [$P2_1/n$; $a = 1.02522(6)$ nm, $b = 1.45736(14)$ nm, $c = 0.90436(6)$ nm, $\beta = 98.36(1)°$]

atom	*x*	*y*	*z*
C(1)	−0.188(4)	0.244(1)	−0.443(1)
C(2)	−0.233(4)	0.232(1)	−0.593(2)
C(3)	−0.029(5)	0.367(1)	0.128(2)
C(4)	0.005(4)	0.418(1)	0.258(2)
C(5)	−0.175(2)	0.077(1)	−0.429(1)
C(6)	−0.160(2)	0.163(1)	−0.362(1)
C(7)	−0.229(3)	0.068(1)	−0.579(1)
C(8)	−0.256(3)	0.148(1)	−0.660(1)
C(9)	−0.120(4)	0.011(1)	−0.318(1)
C(10)	−0.012(5)	0.273(1)	0.141(2)
C(11)	0.037(4)	0.232(1)	0.276(1)
C(12)	0.068(4)	0.283(1)	0.405(2)
C(13)	0.053(4)	0.377(1)	0.391(2)
C(14)	−0.031(4)	0.199(1)	0.031(1)
C(15)	−0.112(3)	0.147(1)	−0.205(1)
C(16)	0.048(1)	0.134(1)	0.247(1)
N(1)	−0.0787(9)	0.055(1)	−0.185(1)
N(2)	0.0059(9)	0.117(1)	0.098(1)
N(3)	0.105(3)	0.076(1)	0.348(1)
N(4)	−0.089(4)	0.214(1)	−0.107(2)
Cl(1)	0.1870(5)	0.027(1)	−0.057(1)
Si(1)	0	0	0

axis. It is clear that the presence of the chlorine atoms prevents extensive π-stacking of neighboring molecules.

3.2. Multilayers. We now turn to the STM studies of the $SiPcCl_2$ film on the H-passivated Si(111) surface. Figure 4 shows a 500 nm × 500 nm STM image of the H-passivated Si(111) surface before deposition of $SiPcCl_2$. A sequence of zigzag steps is clearly resolved, with an average terrace width of about 150 nm, which is a typical morphology of the H-passivated Si(111) surface. On the wide terraces, the corrugation (defined as twice the standard deviation from the mean height) is measured to be about 0.3 nm, indicating a very flat surface. No special features are present on the terraces. Figure 5 shows thick 3D cluster islands of $SiPcCl_2$ which were deposited onto the surface from the 1:3 solution. Clusters with a long axis of 5.5 nm and a short axis of 4.5 nm are clearly visible in the figure, and these clusters appear to stack partially on top of each other along the direction CD. Since the $SiPcCl_2$ molecule is not planar, coaxial face-to-face stacking to form molecular columns (as observed for CuPc on surfaces) is unlikely. The corresponding surface profiles measured along AB and CD in Figure 5, after image background corrections, show a flat cluster top and a sawtooth contour, respectively. As the surface is H-passivated, the interaction between the molecules and the surface is expected to be comparatively weak (as confirmed by the STM manipulation and well-ordered

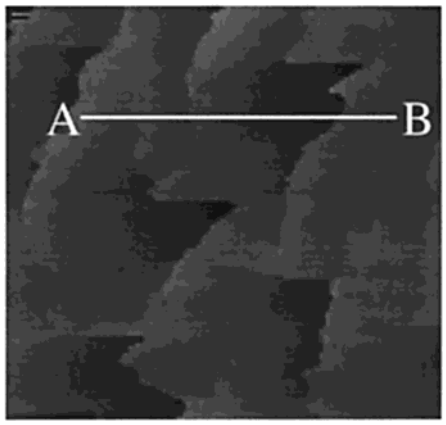

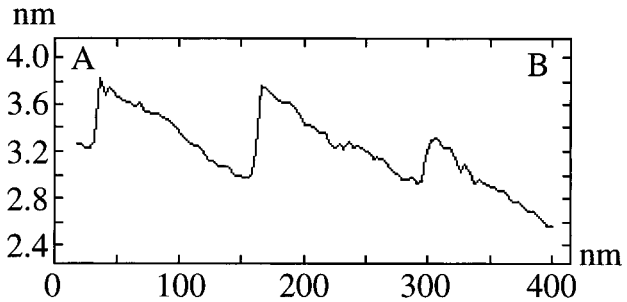

Figure 4. 500 nm × 500 nm STM image of the H-passivated Si(111) surface before the deposition of $SiPcCl_2$. Tunneling conditions: $V = +1.680$ V, $I = 0.35$ nA, constant current mode. A sequence of zigzag steps is clearly resolved, with an average terrace width of about 150 nm. On the wide terraces, the corrugation is measured to be about 0.3 nm, which indicates a very flat surface.

monolayers discussed below), and it may then be expected that the structure of the clusters should resemble the bulk crystal structure to some extent. From the surface profile measured along CD in Figure 5, the cluster top plane tilt angle θ is estimated to be about 22°, which is close to the calculated tilt angle 26° when a single molecule is positioned on a surface (with one Cl atom and the edge of the Pc plane in contact with the surface). The cluster thickness (i.e., the distance EF in Figure 5) is calculated to be about 2.8 nm. Since the distance EF is just measured along the contours of the top of the film (not measured from the H-passivated Si(111) surface), the actual thickness of the film measured from H-passivated Si(111) should be larger than 2.8 nm, which is clearly larger than the corrugation of 0.3 nm determined for a clean H-passivated Si(111) surface. Thus, the features observed in Figure 5 are genuinely due to the deposition of the $SiPcCl_2$ film, and not due to the corrugation of the H-passivated Si(111) surface itself. Bearing in mind the bulk crystal structure and comparing the estimated values from the surface profile measured along CD with the bulk structure, careful consideration of a number of possible stacking arrangements, including those with the Si−Cl bonds parallel to the surface, leads us to the model shown in Figure 6. Each cluster visible in Figure 5 consists of an orthogonal arrangement of 20 molecules arranged in a 4 × 5 array and five layers. These clusters stack one after another on the surface. The normal to the Pc plane of the molecule is tilted away from the normal to the surface, as expected from the fact that the $SiPcCl_2$ molecule is nonplanar. The model then reproduces the contour profiles observed in Figure 5. This type of arrangement can be visualized by looking at the arrangement in the crystal structure in Figure 3, showing that the model is closely similar to the molecular arrangement in the bulk crystal. We can show the degree of similarity by estimating the distances

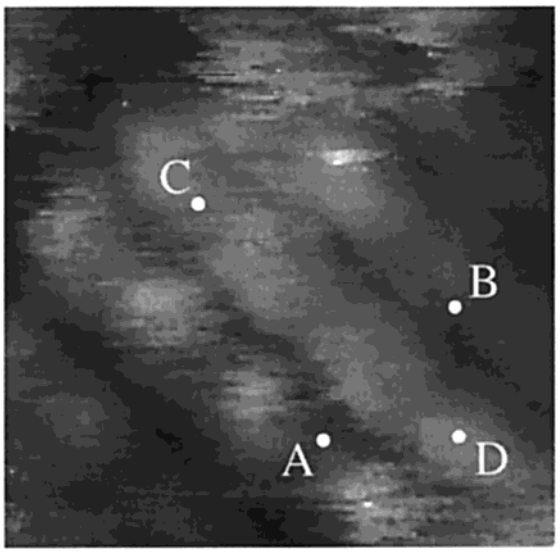

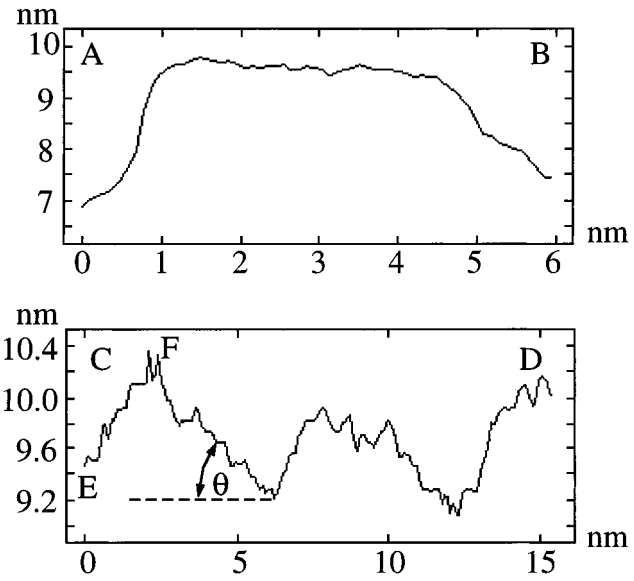

Figure 5. 25 nm × 25 nm STM image of 3D cluster islands of $SiPcCl_2$ on the H-passivated Si(111) surface. Tunneling conditions: $V = +1.680$ V, $I = 0.35$ nA, constant current mode. Clusters with sizes of about 5.5 nm × 4.5 nm are visible. Corresponding surface profiles along AB and CD suggest that the clusters probably consist of molecules that are tilted at the surface.

between atoms of neighboring molecules. Using the STM model, the closest approach of the C(ring) atoms and the nearest Cl atom on a neighboring molecule is estimated to be ca. 0.45 nm, and the closest Cl···Cl approach between Cl atoms of molecules in the staggered layers is estimated to be ca. 0.86 nm. These distances compare favorably with the corresponding intermolecular distances in the crystal structure [C(ring)···Cl, 0.50 nm; Cl···Cl, 0.90 nm].

3.3. Monolayers. In an attempt to obtain monolayers on the surface, we tried to remove the top 3D cluster islands by direct manipulation with the STM tip as done previously for C_{60} films on the same surface.[46] However, this manipulation resulted in cluster islands and vast uncovered areas of silicon surface as shown in Figure 7. By this method, it was not possible to remove just the top layers to obtain thin and stable layers close to the surface. In the case of C_{60}, the intermolecular force is relatively weak, allowing the tip to skim away top layers of C_{60} molecules in thick films, resulting in a flat film after several scans of the

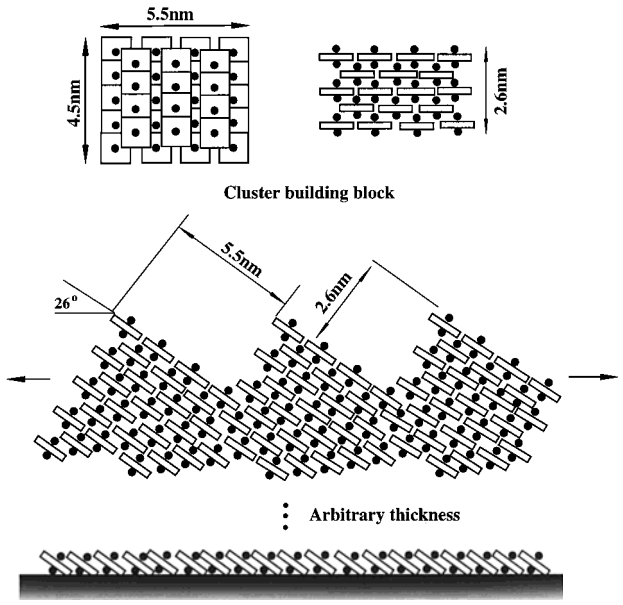

Figure 6. Proposed cluster structure of $SiPcCl_2$ molecules with a size of 5.5 nm × 4.5 nm and a thickness of 2.6 nm, which forms building blocks in thick layers. These clusters are partially stacked and tilted on the H-passivated Si(111) surface.

STM tip over the scan area. The fact that this behavior is not observed for $SiPcCl_2$ leads us to conclude that the intermolecular forces are considerably higher. In Figure 7, well-ordered features are observed: the diameter of each feature is about 1.2 nm, in agreement with the lateral size of the Pc plane in a single molecule.[19,22] Thus, we believe that these features represent individual $SiPcCl_2$ molecules. On top of the first layer, the incomplete second layer (comprising only a few molecules, and indicated with an arrow) is also visible. The four lobes of the molecule are not visible in the STM images. Although there are several reports of studies in which the lobes of phthalocyanine molecules have been resolved in air,[47−49] none of these studies was carried out on a phthalocyanine chloride derivative, and it is possible that the large chlorine atom dominates the images in the present case. The height of one monolayer is measured to be about 0.6 nm along AB as shown in the corresponding surface profile, which is very close to the value of 0.54 nm calculated from our space-filling model with the molecule tilted on the surface (i.e., with one Cl atom and the edge of the Pc plane in contact with the surface), i.e., the distance along the surface normal from the surface to the furthest edge of the Pc plane is estimated to be 0.54 nm. The surface profiles measured along CD and EF show that the separations (center to center) between the neighboring molecules are about 0.8 and 1.4 nm, respectively. These values are in reasonable agreement with the bulk crystal structure (0.90 and 1.46 nm, respectively), suggesting that aspects of the bulk crystal structure are still retained when the molecules are adsorbed on the H-passivated Si(111) surface. The observation of well-ordered $SiPcCl_2$ layers on the surface further confirms the weak interaction between the molecules and the surface.

3.4. Scanning Tunneling Spectroscopy. We have used the scanning tunneling spectroscopy (STS) I−V curve to investigate the nature of the $SiPcCl_2$ films on the surface. The I−V curve (Figure 8) measured in the ordered area in Figure 7 shows marked rectifying behavior. This behavior was duplicated at all points tested over both the monolayer and multilayer films; no local states were observed at different positions on the films. Such rectifying behavior has been observed by Pomerantz et al.[20] and Ottaviano et al.[50] in STS studies of CuPc on graphite

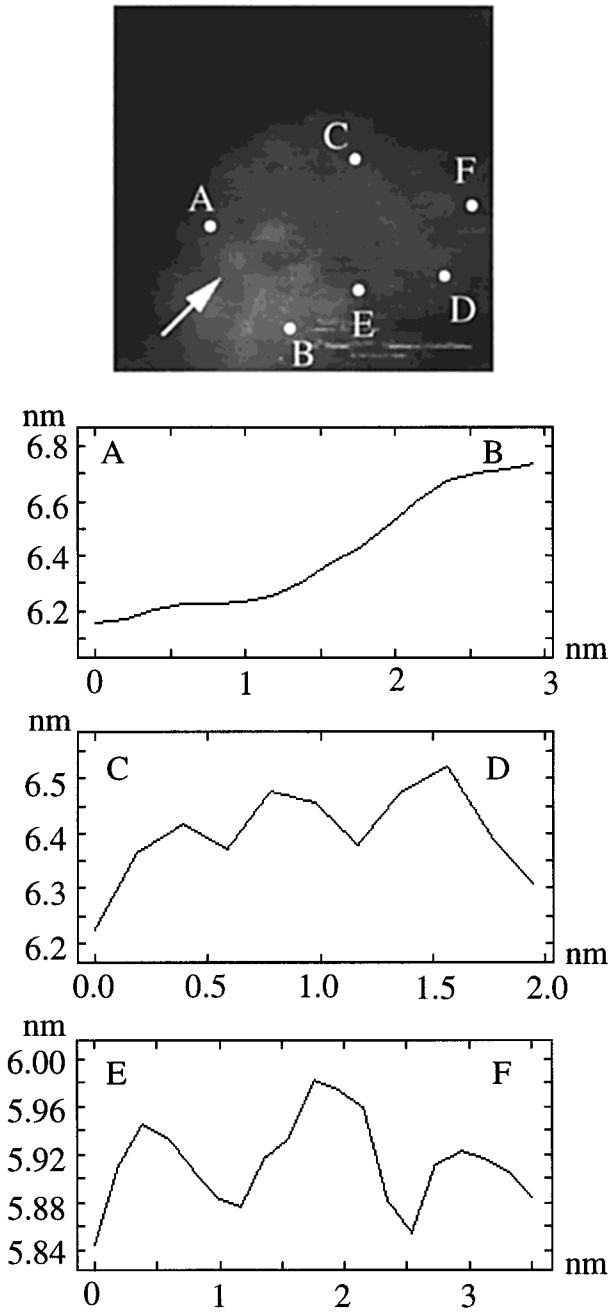

Figure 7. 5 nm × 5 nm STM image of a separated cluster island of $SiPcCl_2$ molecules on the H-passivated Si(111) surface. Tunneling conditions: $V = +1.680$ V, $I = 0.35$ nA, constant current mode. Well-ordered layers are visible in the image. Corresponding surface profiles show that the thickness of one monolayer is about 0.6 nm (along AB). The distances of the neighboring molecules are 1.4 nm (along EF) and 0.8 nm (along CD). These measurements are in agreement with features observed in the bulk crystal structure shown in Figure 3.

and NiPc on Si(111), respectively. This behavior is to be expected for a film that acts as an organic p-type semiconductor (due to oxygen doping) on a p-doped semiconductor surface. We note that the STS behavior is very similar to that of the clean H-passivated Si(111) surface[40] and conclude that in this case the properties of the surface dominate the STS characteristics.

4. Concluding Remarks

The behavior of $SiPcCl_2$ molecules deposited on the H-passivated Si(111) surface has been investigated. Clusters of about 5.5 nm × 4.5 nm in size are observed in high-coverage films, whereas well-ordered individual molecules are observed in low-coverage films. The modeling of the stacking on the surface in high-coverage films is greatly assisted by reference to the bulk crystal structure of $SiPcCl_2$, which we have determined directly from powder X-ray diffraction data using the Monte Carlo method for structure solution. A surface stacking model has been proposed which is consistent with surface profile measurements on the surface layers and consistent with the bulk crystal structure. We deduce that the interaction between the molecules and surface is weaker than the intermolecular attraction, based on attempts to manipulate thick layers on the surface using the STM tip. From scanning tunneling spectroscopy, the $SiPcCl_2$ layers on the H-passivated Si(111) surface exhibit rectifying behavior, which is dominated by the rectifying nature of the H-passivated Si(111) surface rather than any intrinsic rectifying behavior of the $SiPcCl_2$ molecule.

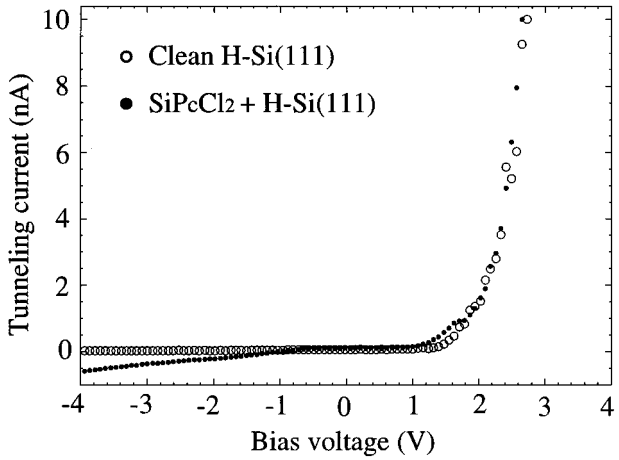

Figure 8. I−V curve (dark dots) measured in the $SiPcCl_2$ monolayers on the H-passivated Si(111) surface in Figure 7 and I−V curve (open circles) measured on a clean H-passivated Si(111) surface (without $SiPcCl_2$ deposited). Both systems show similar rectifying behavior.

Acknowledgment. P.M. is grateful to the School of Physics and Astronomy for awarding a Ph.D. studentship. We also thank C. E. J. Mitchell for a critical reading of the manuscript. This work was supported by the Engineering and Physical Sciences Research Council.

References and Notes

(1) Forrest, S. R.; Burrows, P. E.; Haskal, E. I.; So, F. F. *Phys. Rev.* **1993**, *B49*, 11309.
(2) Matthias, B.; Berndt, R.; Schneider, W. D. *Phys. Rev.* **1996**, *B55*, 1384.
(3) Chakrabarti, A.; Schmidt, A.; Valencia, V.; Fluegel, B.; Mazumdar, S.; Armstrong, N.; Peyghambarian, N. *Phys. Rev.* **1997**, *B57*, R4205.
(4) Hiromitsu, I.; Yamamoto, H.; Ito, T. *Phys. Rev.* **1995**, *B52*, 7252.
(5) Poirier, M.; Pouget, J. P.; Thompson, J. A.; Hoffman, B. M. *Phys. Rev.* **1995**, *B51*, 14861.
(6) Murata, K.; Ito, S.; Takahashi, K.; Hoffman, B. M. *Appl. Phys. Lett.* **1996**, *68*, 427.
(7) Bao, Z.; Lovinger, A. J.; Dodabalapur, A. *Appl. Phys. Lett.* **1996**, *69*, 3066.
(8) Parthasarathy, G.; Burrows, P. E.; Khalfin, V.; Kozlov, V. G.; Forrest, S. R. *Appl. Phys. Lett.* **1998**, *72*, 2138.
(9) Kanbara, H.; Maruno, T.; Yamashita, A.; Matsumoto, S.; Hayashi, T.; Konami, H.; Tanaka, N. *Appl. Phys. Lett.* **1996**, *80*, 3674.
(10) Yanagi, H.; Imamura, M.; Ashida, M. *J. Appl. Phys.* **1994**, *75*, 2061.
(11) Brynda, E.; Koropecky, I.; Kalvoda, L.; Nespurek, S. *Thin Solid Films* **1990**, *199*, 375.
(12) Robertson, J. M. *J. Chem. Soc.* **1935**, 615.
(13) Hua, Y. L.; Jiang, D. P.; Shu, Z. Y.; Petty, M. C.; Roberts, G. G.; Ahmad, M. M. *Thin Solid Films* **1990**, *192*, 383.

(14) He, J.; Larkin, H. E.; Li, Y. S.; Rihter, B. D.; Zaidi, S. I. A.; Rodgers, M. A. J.; Mukhter, H.; Kenney M. E.; Oleinick, N. L. *Photochem. Photobiol.* **1997**, *65*, 581.

(15) BenHur, E.; Oetjen, J.; Horowitz, B. *Photochem. Photobiol.* **1997**, *65*, 456.

(16) Anderson, C.; Hrabovsky, S.; McKinley, Y.; Tubesing, K.; Tang, H. P.; Dunbar, R.; Mukhtar, H.; Elmets, C. A. *Photochem. Photobiol.* **1997**, *65*, 895.

(17) Mächler, E.; Arrouy, F.; Fritsch, E.; Bednorz, J. G.; Berke, H.; Huber, J. R.; Locquet, J. P. *Appl. Phys. Lett.* **1997**, *71*, 710.

(18) Nakamura, M.; Morita, Y.; Mori, Y.; Ishitani, A.; Tokumoto, H. *J. Vac. Sci. Technol.* **1996**, *B14*, 1109.

(19) Maeda, Y.; Matsumoto, T.; Kasaya, M.; Kawai, T. *Jpn. J. Appl. Phys.* **1996**, *35*, L405.

(20) Pomerantz, M.; Aviram, A.; McCorkle, R. A.; Li, L.; Schrott, A. G. *Science* **1992**, *255*, 1115.

(21) Tanaka, H.; Kawai, T. *Jpn. J. Appl. Phys.* **1996**, *35*, 3759.

(22) Rochet, F.; Dufour, G.; Roulet, H.; Motta, N.; Sgarlata, A.; Piancastelli, M. N.; Crescenzi, M. D. *Surf. Sci.* **1994**, *319*, 10.

(23) Kanai, M.; Kawai, T.; Motai, K.; Wang, X. D.; Hashizume, T.; Sakura, T. *Surf. Sci.* **1995**, *329*, L619.

(24) Strohmaier, R.; Ludwig, C.; Petersen, J.; Gomph, B.; Eisenmenger, W. *J. Vac. Sci. Technol.* **1996**, *B14*, 1079.

(25) Lu, X.; Hipps, K. W. *J. Phys. Chem.* **1997**, *B101*, 5391.

(26) Yanagi, H.; Mikami, T.; Terui, T.; Mashiko, S. *J. Appl. Phys.* **1997**, *81*, 7306.

(27) Dirk, C. W.; Inabe, T.; Schoch, K. F., Jr.; Marks, T. J. *J. Am. Chem. Soc.* **1983**, *105*, 1539.

(28) Miao, P.; Robinson, A. W.; Palmer, R. E. *J. Phys. D: Appl. Phys.* **1998**, *31*, L37.

(29) Harris, K. D. M.; Tremayne, M. *Chem. Mater.* **1996**, *8*, 2554.

(30) Harris, K. D. M.; Tremayne, M.; Lightfoot, P.; Bruce, P. G. *J. Am. Chem. Soc.* **1994**, *116*, 3543.

(31) Tremayne, M.; Kariuki, B. M.; Harris, K. D. M. *Angew. Chem., Int. Ed. Engl.* **1997**, *36*, 770.

(32) Elizabé, L.; Kariuki, B. M.; Harris, K. D. M.; Tremayne, M.; Epple, M.; Thomas, J. M. *J. Phys. Chem.* **1997**, *B101*, 8827.

(33) Andreev, Y. G.; Lightfoot, P.; Bruce, P. G. *J. Chem. Soc., Chem. Commun.* **1996**, 2169.

(34) Andreev, Y. G.; MacGlashan, G. S.; Bruce, P. G. *Phys. Rev.* **1997**, *B55*, 12011.

(35) David, W. I. F.; Shankland, K.; Shankland, N. *Chem. Commun.* **1998**, 931.

(36) Kariuki, B. M.; Serrano-González, H.; Johnston, R. L.; Harris, K. D. M. *Chem. Phys. Lett.* **1997**, *280*, 189.

(37) Shankland, K.; David, W. I. F.; Csoka, T. *Z. Krist.* **1997**, *212*, 550.

(38) Harris, K. D. M.; Johnston, R. L.; Kariuki, B. M. *Acta Crystallogr.* **1998**, *A54*, 632.

(39) Kariuki, B. M.; Calcagno, P.; Harris, K. D. M.; Philp, D.; Johnston, R. L. *Angew. Chemie, Int. Ed. Engl.* **1999**, *38*, 831.

(40) Miao, P.; Robinson, A. W.; Palmer, R. E. *J. Phys. D: Appl. Phys.*, in press.

(41) Visser, J. W. *J. Appl. Crystallogr.* **1969**, *2*, 89.

(42) Tremayne, M.; Kariuki, B. M.; Harris, K. D. M. *OCTOPUS, Monte Carlo Technique for Powder Structure Solution*, 1997.

(43) Larson, A. C.; von Dreele, R. B. Los Alamos Lab. Report No. LA-UR-86-748, 987.

(44) Allen, F. H.; Johnson, O. *Chem. Design Automation News* **1993**, *8*, 130.

(45) Allen, F. H.; Kennard, O.; Watson, D. G.; Brammer, L.; Orpen, A. G. *J. Chem. Soc., Perkin Trans 2*, **1987**, S1.

(46) Miao, P.; Robinson, A. W.; Palmer, R. E. *J. Phys. D: Appl. Phys.* **1997**, *30*, 3307.

(47) Lippel, P. H.; Wilson, R. J.; Miller, M. D.; Woll, C.; Chiang, S. *Phys. Rev. Lett.* **1989**, *62*, 171.

(48) Ludwig, C.; Strohmaier, R.; Petersen, J.; Gompf, B.; Eisenmenger, W. *J. Vac. Sci. Technol.* **1994**, *B12*, 1963.

(49) Fritz, T.; Hara, M.; Knoll, W.; Sasabe, H. *Mol. Cryst. Liq. Cryst.* **1994**, *A252*, 561.

(50) Ottaviano, L.; Santucci, S.; Di Nardo, S.; Lozzi, L.; Passacantando, M.; Picozzi, P. *J. Vac. Sci. Technol.* **1997**, *15*, 1014.